



MATH 552: preliminary dissertation

---

**Mathematical analysis of epithelial  
tissue topology**

---

Author:

Nouf Alghamdi

Supervisor:

Dr. Bakhtier Vasiev

May 20, 2016

# Contents

<b>1</b>	<b>Summary</b>	<b>2</b>
<b>2</b>	<b>Introduction</b>	<b>3</b>
2.1	Biological background . . . . .	3
2.2	Review of models describing epithelial tissue topology . . . . .	4
2.2.1	GPNP (Gibson's) model . . . . .	4
2.2.2	Newman's first model . . . . .	6
2.2.3	Newman's second model . . . . .	7
2.2.4	Newman's third model . . . . .	8
2.3	Conclusion . . . . .	8
<b>3</b>	<b>Analysis of models' transition matrices.</b>	<b>10</b>
3.1	Eigenvalues and eigenvectors of the transition matrices . . . . .	11
3.1.1	(GPNP) model . . . . .	11
3.1.2	Newman's first model . . . . .	12
3.1.3	Newman's second model . . . . .	13
3.1.4	Newman's third model . . . . .	15
3.2	Conclusion . . . . .	16
<b>4</b>	<b>Fitting the experimental histogram to commonly used probability density functions.</b>	<b>18</b>
4.1	Poisson distribution . . . . .	18
4.2	Normal distribution . . . . .	19
4.3	Log-normal distribution . . . . .	21
4.4	Conclusion . . . . .	22
<b>5</b>	<b>Future work</b>	<b>24</b>

# Chapter 1

## Summary

For over a century topology concepts were used to study, explain and organise several structures that develop from comparatively natural physical processes, for instance, honeycombs, drying mud and even geological features of extra-terrestrial lunar surfaces [13]. More recently, Gibson and Newman (2006-2011) [2], [7], were fascinated by the emergence of geometric order in the two-dimensional structure of epithelial cells. That was the motive behind the construction of four different models. They compute the topology of tissue by the distribution of a number of neighbour and geometry of tissue by the distribution of cell shapes and sizes. Each and every one of them was built on different assumptions and had advantages and disadvantages. In addition, the mathematical study and analysis of these models highlighted a significant number of problems in these models. Some of these problems have been addressed mathematically and some issues were not solved because it was basically built on assumptions. This report will: briefly review these models and outline the main points and aspects that were based on these models. In addition, analyses the transition matrices of each model by solving eigen-problems. Furthermore, attempt to find a propitiate probability function which could describe this pattern by fitting the experimental histogram which was obtained from actual observation to the commonly used probability density functions.

Therefore, the aim of this report is to review and analyse these models from a mathematical point of view.

# Chapter 2

## Introduction

### 2.1 Biological background

The smallest component of the body is known as the cell. A group of cells formed the tissue. There are four primary types of tissues: epithelial, connective, muscular, and nervous tissue. Under each primary tissue, there might be several sub-tissues. Each tissue has different functions. The general concept of cells and tissues regarding the structure and its vital functions, such as signal transmission, are carried out by pure biology [6]. However, recently there were some cases where biology was unable to explain clearly some of the phenomena and patterns prompting scientists to use topological concepts in order to organise, translate and analyse these patterns. This report will focus on one particular type of these tissues. The epithelial tissue, which represents the lining of the internal organs such as the stomach and covers the outer surface of the body (skin). [1] [8] [9] [10].

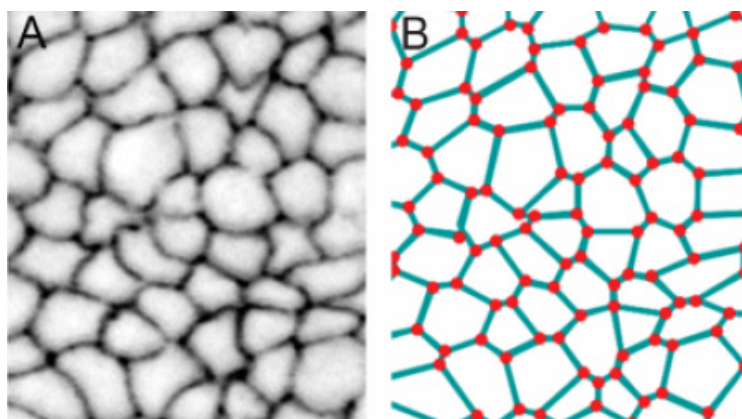


Figure 2.1: A: Microscopic view shows polygonal topology of the *Drosophila* wing. B: Diagram of the extracted polygonal network from A [13].

The focus on this type of tissue for several reasons: The epithelial is usually a 2-dimensional array of cells. Also through a microscopic study of epithelial tissue in various organisms such as *Drosophila* (a fruit fly), *Xenopus* (a frog) and *Hydra* (a tiny fresh-water relative of jellyfish), it was found that an identical, asymmetric distribution of polygonal shapes shows up over these organisms.

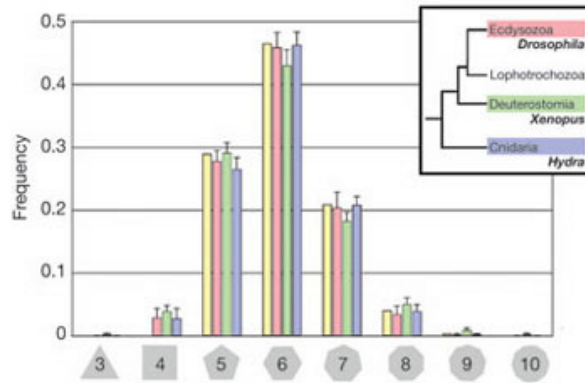


Figure 2.2: *Drosophila* wing disc (pink), *Xenopus* tail epidermis (green) and *Hydra* epidermis (blue) all exhibit a similar non-gaussian distribution of epithelial polygons with less than 50% hexagonal cells and high (and asymmetric) percentages of pentagonal and heptagonal cells. The inset indicates relative phylogenetic positions for *Drosophila*, *Xenopus* and *Hydra* [4].

## 2.2 Review of models describing epithelial tissue topology

There were several attempts to produce models describing the topology of epithelial tissue. Perhaps the most well-known were the one that produced by Gibson (2006) in (The emergence of geometric order in proliferating metazoan epithelia) [2].

### 2.2.1 GPNP (Gibson's) model

Gibson's model was based on some assumptions [2].

- [1] Cells have a polygonal shape, where the minimum number of the (edges-vertices) in each cell is four.
- [2] Divisions through vertices of the mother cell neglected in contrast to the divisions that occur through sides.
- [3] Cells divide randomly.
- [4] Cells divide synchronously.
- [5] Spatial correlations between the sidedness of cells can be neglected.

#### The model:

The main idea of Gibsons algorithm was about a mother cell with ( $i$ )-sides divides into two daughters, placing two (vertices-edges) from the mother cell in each side of the division line, which leaves ( $i - 4$ ) edges in the mother cell to be distributed randomly. While the gaining (vertices-edges) by the daughters with ( $j$ )-sides from each division will be four, 2 from the mother cell and the other two will be given by the division line, which leaves ( $j - 4$ ) edges in the daughter cell to be gained randomly. This random separation follows the binomial distribution.

Therefore, the random probabilities of given (the mother) and gaining (the daughters) edges is given by:

$$T_{i,j} = \frac{(i-4)!}{(j-4)!(i-j)!} * \frac{1}{2^{(i-4)}} \quad (2.1)$$

$$T_{i,j} = \begin{bmatrix} 1 & 0 & 0 & 0 & 0 & 0 \\ \frac{1}{2} & \frac{1}{2} & 0 & 0 & 0 & 0 \\ \frac{1}{4} & \frac{1}{2} & \frac{1}{4} & 0 & 0 & 0 \\ \frac{1}{8} & \frac{3}{8} & \frac{3}{8} & \frac{1}{8} & 0 & 0 \\ \frac{1}{16} & \frac{1}{4} & \frac{3}{8} & \frac{1}{4} & \frac{1}{16} & 0 \\ \frac{1}{32} & \frac{5}{32} & \frac{5}{16} & \frac{5}{16} & \frac{5}{32} & \frac{1}{32} \end{bmatrix}$$

Each division will produce six new sides. Four of them will be distributed equally between the two daughters, and to neighbouring cells each being provided with an additional side.

According to Gibsons assumption, the cells divide synchronously and one round of division cannot be completed unless each cell has divided. Therefore, each cell in average will be provided with one additional side after each round of division and this is the role of matrix  $S$ .

$$S_{i,j} = \begin{bmatrix} 0 & 1 & 0 & 0 & 0 & 0 \\ 0 & 0 & 1 & 0 & 0 & 0 \\ 0 & 0 & 0 & 1 & 0 & 0 \\ 0 & 0 & 0 & 0 & 1 & 0 \\ 0 & 0 & 0 & 0 & 0 & 1 \\ 0 & 0 & 0 & 0 & 0 & 0 \end{bmatrix}$$

By multiplying these two matrices we have the transition matrix of GPNP model

$$U = \begin{bmatrix} 0 & 1 & 0 & 0 & 0 & 0 \\ 0 & \frac{1}{2} & \frac{1}{2} & 0 & 0 & 0 \\ 0 & \frac{1}{4} & \frac{1}{2} & \frac{1}{4} & 0 & 0 \\ 0 & \frac{1}{8} & \frac{3}{8} & \frac{3}{8} & \frac{1}{8} & 0 \\ 0 & \frac{1}{16} & \frac{1}{4} & \frac{3}{8} & \frac{1}{4} & \frac{1}{16} \\ 0 & \frac{1}{32} & \frac{5}{32} & \frac{5}{16} & \frac{5}{16} & \frac{5}{32} \end{bmatrix} \rightarrow U^T = \begin{bmatrix} 0 & 0 & 0 & 0 & 0 & 0 \\ 1 & \frac{1}{2} & \frac{1}{4} & \frac{1}{8} & \frac{1}{16} & \frac{1}{32} \\ 0 & \frac{1}{2} & \frac{1}{2} & \frac{3}{8} & \frac{1}{4} & \frac{5}{32} \\ 0 & 0 & \frac{1}{4} & \frac{3}{8} & \frac{3}{8} & \frac{5}{16} \\ 0 & 0 & 0 & \frac{1}{8} & \frac{1}{4} & \frac{5}{16} \\ 0 & 0 & 0 & 0 & \frac{1}{16} & \frac{5}{32} \end{bmatrix}$$

The distribution of different shapes of cells at the current generation is given by the product of the transpose of matrix  $U$  multiplied by the column-vector of the cells in the previous generation.

$$p^{(t)} = U^T * p^{(t-1)} \quad (2.2)$$

on another word

$$p^{(t)} = (U^T)^t * p^{(0)} \quad (2.3)$$

where

$$p^{(t)} = [p_4, p_5, p_6, p_7, p_8, p_9 \dots]^{(t)}$$

$t$  represents the time or generation and  $[4, 5, 6, 7, 8, 9 \dots]$  defined as the state of the cell which represents the number of its sides .  $P_s$  represents the relative frequency of  $s$ -sided cell in the population, and the infinite row vector.

Assuming that

$$p^{(0)} = [0, 0, 1, 0, 0, 0]$$

Inserting the obtained values into 2.3 yields:

	$t = 10$	$t = 100$	$t = 1000$	$t = 10000$	$t = 100000$
$p_4$	0	0	0	0	0
$p_5$	0.28871	0.28656	0.26593	0.12596	0.000071611
$p_6$	0.46384	0.46039	0.42724	0.20237	0.00011505
$p_7$	0.20840	0.20685	0.19195	0.090921	0.000051689
$p_8$	0.035844	0.035576	0.033015	0.015638	0.0000088903
$p_9$	0.0026555	0.0026355	0.0024458	0.0011585	0.00000065861
Sum	0.9994495	0.9920115	0.9205808	0.4360475	0.000247899

Table 1: Evolution of cell-edges distribution in Gibson's model.

### 2.2.2 Newman's first model

In his first modification, Newman [7], changed some of the assumptions in the previous model, to construct his first model which was based on:

[A] Allowing transient 3-sided cells.

[B] Change the mechanisms of the division to be the mother cell gives only one (edge-vertex) to each daughter instead of two.

Obtaining such clear error in the previous model motivate Newman to change the first assumption in Gibsons model, which was about the minimum number of the sides in each cell, to be three this time.

$$T_{i,j} = \frac{(i-2)!}{(j-3)!(i-j+1)!} * \frac{1}{2^{(i-2)}} \quad (2.4)$$

Using the 2.4 formula, the entries of matrix T changed to this form:

$$T_{N1} = \begin{bmatrix} \frac{1}{2} & \frac{1}{2} & 0 & 0 & 0 & 0 & 0 \\ \frac{1}{4} & \frac{1}{2} & \frac{1}{4} & 0 & 0 & 0 & 0 \\ \frac{1}{8} & \frac{3}{8} & \frac{3}{8} & \frac{1}{8} & 0 & 0 & 0 \\ \frac{1}{16} & \frac{1}{4} & \frac{3}{8} & \frac{1}{4} & \frac{1}{16} & 0 & 0 \\ \frac{1}{32} & \frac{5}{32} & \frac{5}{16} & \frac{5}{16} & \frac{5}{32} & \frac{1}{32} & 0 \\ \frac{1}{64} & \frac{3}{32} & \frac{15}{64} & \frac{5}{16} & \frac{15}{64} & \frac{3}{32} & \frac{1}{64} \\ \frac{1}{128} & \frac{7}{128} & \frac{21}{128} & \frac{35}{128} & \frac{35}{128} & \frac{21}{128} & \frac{7}{128} \end{bmatrix}$$

And to continue with the same procedure, the results:

	$t = 10$	$t = 100$	$t = 1000$
$p_3$	0	0	0
$p_4$	0.082838	0.067543	0.0088317
$p_5$	0.26586	0.21682	0.028351
$p_6$	0.33227	0.27108	0.035445
$p_7$	0.21098	0.17222	0.022518
$p_8$	0.076223	0.062265	0.0081415
$p_9$	0.016458	0.013457	0.0017596
The sum	0.984629	0.803385	0.1050468

Table 2: Evolution of cell-edges distribution in Newman's first model.

### 2.2.3 Newman's second model

The concept behind his second model (modification) is to introduce the pure meaning of randomness to Gibsons model [7].

Newman's suggestion concerning randomness issue: the mother cell should be divided randomly except two (edges-vertices), this well lead to three cases:

- 1) If one side of the division has no (edges-vertices) then provide it with this two.
- 2) If one side has only one (edge-vertex) then distribute one randomly if its remain with only one then provide it with that last one otherwise divide randomly.
- 3) If both side of the division line has at least two (edges-vertices) then distribute the rest randomly.

$$T_{i,j} = \frac{i!}{(j-2)!(i-j+2)!} * \frac{1}{2^i - (2i+2)} \quad (2.5)$$

Applying these conditions produced this formula for  $T$  matrix where  $(2i+2)$  represents the discarded probabilities which satisfy Gibson's assumptions. Using the equation 2.5, the entries of matrix T take this form:

$$T_{N_2} = \begin{bmatrix} 1 & 0 & 0 & 0 & 0 & 0 \\ \frac{1}{2} & \frac{1}{2} & 0 & 0 & 0 & 0 \\ \frac{3}{10} & \frac{2}{5} & \frac{3}{10} & 0 & 0 & 0 \\ \frac{3}{16} & \frac{5}{16} & \frac{5}{16} & \frac{3}{16} & 0 & 0 \\ \frac{2}{17} & \frac{4}{17} & \frac{5}{17} & \frac{4}{17} & \frac{2}{17} & 0 \\ \frac{3}{41} & \frac{7}{41} & \frac{21}{82} & \frac{21}{82} & \frac{7}{41} & \frac{3}{41} \end{bmatrix}$$

By following the same procedure as the first model the results at  $t=1000$ :

	$t = 10$	$t = 100$	$t = 1000$	$t = 10000$
$p_4$	0	0	0	0
$p_5$	0.33158	0.31582	0.19406	0.0014889
$p_6$	0.40402	0.38482	0.23646	0.0018142
$p_7$	0.20141	0.19183	0.11787	0.00090437
$p_8$	0.051891	0.049419	0.030366	0.00023299
$p_9$	0.007368	0.0070156	0.0043108	0.000033075
The sum	0.996269	0.9489046	0.5830668	0.004473535

Table 3: Evolution of cell-edges distribution in Newman's second model.



### 2.2.4 Newman's third model

In this model Newman [7], used the same idea as in Newmans second model (Introducing the pure meaning of randomness) except he applied it onto his first model which makes this model based on:

- A) Allowing transient 3-sided cells.
- B) The mother cell will be distributed randomly, and the number of the gained edges by the daughter will be random except the two which will be gained from the cleavage plane.

$$T_{i,j} = \frac{i!}{(j-2)!(i-j+2)!} * \frac{1}{2^i - 2} \quad (2.6)$$

Where  $(-2)$  in  $(2^i - 2)$  represents the discarded probabilities which satisfy his assumptions A and B. With these two conditions the entries of the T matrix changed to be:

$$T_{N3} = \begin{bmatrix} \frac{1}{2} & \frac{1}{2} & 0 & 0 & 0 & 0 & 0 \\ \frac{2}{7} & \frac{3}{7} & \frac{2}{7} & 0 & 0 & 0 & 0 \\ \frac{1}{6} & \frac{1}{3} & \frac{1}{3} & \frac{1}{6} & 0 & 0 & 0 \\ \frac{3}{31} & \frac{15}{62} & \frac{10}{31} & \frac{15}{62} & \frac{3}{31} & 0 & 0 \\ \frac{1}{18} & \frac{1}{6} & \frac{5}{18} & \frac{5}{18} & \frac{1}{6} & \frac{1}{18} & 0 \\ \frac{4}{127} & \frac{14}{127} & \frac{28}{127} & \frac{35}{127} & \frac{28}{127} & \frac{14}{127} & \frac{4}{127} \\ \frac{3}{170} & \frac{6}{85} & \frac{14}{85} & \frac{21}{85} & \frac{21}{85} & \frac{14}{85} & \frac{6}{85} \end{bmatrix}$$

Multiplying this matrix by the  $S$  matrix, transpose the product and insert the final matrix in equation 2.3, yields:

	$t = 10$	$t = 100$	$t = 1000$
$p_3$	0	0	0
$p_4$	0.11789	0.074508	0.00076038
$p_5$	0.24889	0.15732	0.0016055
$p_6$	0.28931	0.1829	0.0018666
$p_7$	0.1971	0.12464	0.001272
$p_8$	0.086393	0.054655	0.00055777
$p_9$	0.024642	0.015598	0.00015918
The sum	0.964225	0.609621	0.00622143

Table 4: Evolution of cell-edges distribution in Newman's third model.

## 2.3 Conclusion

This figure 2.3 has shown the results of four different approaches compared to the results that were obtained from experimental observation for various types of organisms. These attempts have tried to establish an accurate model by using topology and focusing on the shape of the cells. It can be seen in Figure 2.3 that, Gibson [2], had shown a significant approximation. His model has failed to show one type of

cells (4-sided cells) after one round of division. Such defect was caused by his assumptions and the role of matrix  $S$ .

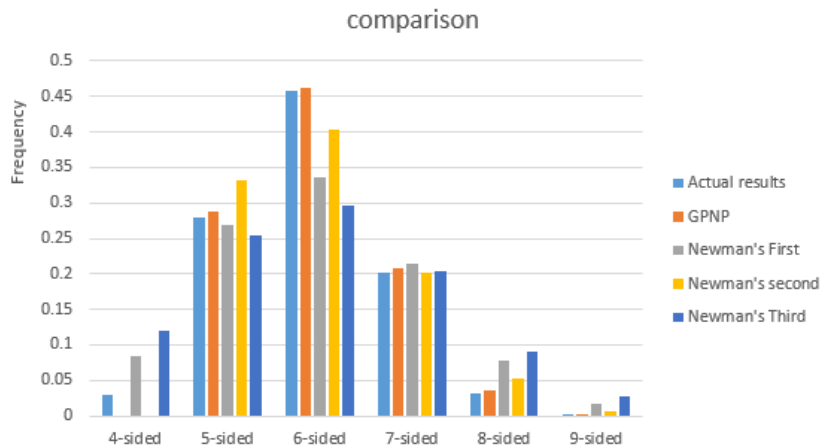


Figure 2.3: The comparison between cell-edges distribution of experimental observation, Gibson's model, Newman's first, second and third modification.

Newman [7], investigated Gibson's model and started by re-examining Gibson's assumptions. That led to construct three models by adjusting some factors. According to Figure 2.3, in the first modification, Newman manages to deliver four-sided cells in the mathematical calculation as in the experimental observation. However, that appearance was at the expense of other shapes proportion. In the second and third modifications, the pure meaning of randomness "as he argued" which was applied to Gibson's model and Newman's first model led to an even worse agreement.

## Chapter 3

# Analysis of models' transition matrices.

There was another gap noted in the previous models which are the fact that as  $t \rightarrow \infty$  the vector  $p^{(t)} \rightarrow 0$  and the sum of the vector  $p^{(t)} \ll 1$ . So, each time the vector needed to be normalised in order to obtain the values and to avoid convergence to zero.

**Example.**

$t = 100000$	(GNPN) model	Normative (GNPN) model
$p_4$	0	0
$p_5$	0.000071611	0.288871782
$p_6$	0.00011505	0.464100467
$p_7$	0.000051689	0.208508379
$p_8$	0.0000088903	0.035862602
$p_9$	0.00000065861	0.002656768
The sum	0.000247899	1

Table 5: Illustration of (GNPN) model at  $t= 100000$ , before and after being normalized.

Moreover, this gap was caused by: The role of the matrix  $S$  which was the main reason of such leak. The concept of matrix  $S$  is to add one extra edge to each cell after one round of division which means that when 9 – sided cell gained one extra edge, it will be lost from the transition matrix  $U = (T.S)$ . In another word because of the matrix  $S$  the probability of 9 – sided cell to remain 9 – sided cell after one round of division = 0. Due to that if the same size of the matrix  $U$  were obtained every time the leak can be seen. To eliminate the leak matrix  $S$  was modified to be in this form:

$$S_{i,j} = \begin{bmatrix} 0 & 1 & 0 & 0 & 0 & 0 \\ 0 & 0 & 1 & 0 & 0 & 0 \\ 0 & 0 & 0 & 1 & 0 & 0 \\ 0 & 0 & 0 & 0 & 1 & 0 \\ 0 & 0 & 0 & 0 & 0 & 1 \\ 0 & 0 & 0 & 0 & 0 & 1 \end{bmatrix}$$

That means each type of the cell will gain one extra edge from dividing neighbour except the 9-sided type, to make sure that such type will remain in the transition matrix after the division. Hence, the obtained transition matrix will be in this form:

$$U = \begin{bmatrix} 0 & 1 & 0 & 0 & 0 & 0 \\ 0 & \frac{1}{2} & \frac{1}{2} & 0 & 0 & 0 \\ 0 & \frac{1}{4} & \frac{1}{2} & \frac{1}{4} & 0 & 0 \\ 0 & \frac{1}{8} & \frac{3}{8} & \frac{3}{8} & \frac{1}{8} & 0 \\ 0 & \frac{1}{16} & \frac{1}{4} & \frac{3}{8} & \frac{1}{4} & \frac{1}{16} \\ 0 & \frac{1}{32} & \frac{5}{32} & \frac{5}{16} & \frac{5}{16} & \frac{3}{16} \end{bmatrix}$$

Thus, the sum of the coefficients of each row in matrix  $U$  or the sum of the coefficients of each column in matrix  $(U)^T$  is equal to one, on contrary of the previous transition matrices where the sum of the last (row-column) was  $< 1$

Inserting the modified matrix  $(U)^T$  in all previous models, yields:

$t = 1000$	(GPNP) model	N1 model	N2 model	N3 model
$p_4$	0	0.0834699	0	0.1204276
$p_5$	0.2887968	0.2682236	0.33234474	0.2548167
$p_6$	0.4640083	0.3360083	0.4050672	0.2973409
$p_7$	0.2085275	0.2143541	0.20215874	0.2041609
$p_8$	0.0359054	0.0782208	0.0522927	0.0908377
$p_9$	0.002762	0.0197232	0.00813662	0.0324163
The sum	1	1	1	1

Table 6: Stable cell-edges distribution in the models after adjusting matrix  $S$ .

### 3.1 Eigenvalues and eigenvectors of the transition matrices

This part of the chapter analyses the transition matrices of the previous models by solving eigen-problems.

#### 3.1.1 (GPNP) model

The transition matrix  $(U)^T$  of Gibsons model: 4, 5, 6, 7, 8, 9-sided cells.

$$U^T = \begin{bmatrix} 0 & 0 & 0 & 0 & 0 & 0 \\ 1 & \frac{1}{2} & \frac{1}{4} & \frac{1}{8} & \frac{1}{16} & \frac{1}{32} \\ 0 & \frac{1}{2} & \frac{1}{2} & \frac{3}{8} & \frac{1}{4} & \frac{5}{32} \\ 0 & 0 & \frac{1}{4} & \frac{3}{8} & \frac{3}{8} & \frac{5}{16} \\ 0 & 0 & 0 & \frac{1}{8} & \frac{1}{4} & \frac{5}{16} \\ 0 & 0 & 0 & 0 & \frac{1}{16} & \frac{3}{16} \end{bmatrix}$$

The characteristic equation of the transition matrix:

$$\lambda^6 - \frac{29\lambda^5}{16} + \frac{253\lambda^4}{256} - \frac{95\lambda^3}{512} + \frac{161\lambda^2}{16384} - \frac{\lambda}{16384} = 0 \quad (3.1)$$

Solving equation 3.1, gives this eigenvalues:

$$\text{Eigenvalues} = \begin{bmatrix} 1.000 \\ 0.4989129 \\ 0.2328268 \\ 0.07362346 \\ 0.007136843 \\ 0 \end{bmatrix}$$

The eigenvectors corresponding to this eigenvalues:

$$\begin{bmatrix} 0 & 0 & 0 & 0 & 0 & 0.0121 \\ 0.4928 & -0.6297 & 0.4999 & -0.2498 & -0.0589 & -0.1091 \\ 0.7917 & -0.3800 & -0.2478 & 0.5401 & 0.3236 & 0.3880 \\ 0.3558 & 0.5591 & -0.7495 & 0.0274 & -0.6734 & -0.6790 \\ 0.0613 & 0.3753 & 0.2091 & -0.7041 & 0.6255 & 0.5820 \\ 0.0047 & 0.0753 & 0.2883 & 0.3865 & -0.2168 & -0.1940 \end{bmatrix}$$

By choosing the eigenvector that corresponding to the eigenvalue 1, and normalising this eigenvector, yields:

$\lambda = 1$	Eigenvector
$p_4$	0
$p_5$	0.2887968
$p_6$	0.4640083
$p_7$	0.2085275
$p_8$	0.0359054
$p_9$	0.002761954
The sum	1

Table 7: Cell-edges distribution as represented by eigenvector corresponding to  $\lambda = 1$  in (GPNP) model.

This is the same results that were obtained from Gibson's model.

### 3.1.2 Newman's first model

The transition matrix  $(U)^T$  of Newman's first model: 3, 4, 5, 6, 7, 8, 9-sided cells.

$$U^T = \begin{bmatrix} 0 & 0 & 0 & 0 & 0 & 0 & 0 \\ \frac{1}{2} & \frac{1}{4} & \frac{1}{8} & \frac{1}{16} & \frac{1}{32} & \frac{1}{64} & \frac{1}{128} \\ \frac{1}{2} & \frac{1}{2} & \frac{3}{8} & \frac{1}{4} & \frac{5}{32} & \frac{3}{32} & \frac{7}{128} \\ 0 & \frac{1}{4} & \frac{3}{8} & \frac{3}{8} & \frac{5}{16} & \frac{15}{64} & \frac{21}{128} \\ 0 & 0 & \frac{1}{8} & \frac{1}{4} & \frac{5}{16} & \frac{5}{16} & \frac{35}{128} \\ 0 & 0 & 0 & \frac{1}{16} & \frac{5}{32} & \frac{15}{64} & \frac{35}{128} \\ 0 & 0 & 0 & 0 & \frac{1}{32} & \frac{7}{64} & \frac{29}{128} \end{bmatrix}$$

The characteristic equation of the transition matrix:

$$\lambda^7 - \frac{113 \lambda^6}{64} + \frac{7497 \lambda^5}{8192} - \frac{10273 \lambda^4}{65536} + \frac{30743 \lambda^3}{4194304} - \frac{921 \lambda^2}{16777216} + \frac{3 \lambda}{134217728} = 0 \quad (3.2)$$

Solving equation 3.2, gives this eigenvalues:

$$Eigenvalues = \begin{bmatrix} 1.0000 \\ 0.4926396 \\ 0.2099667 \\ 0.06100359 \\ 0.009320917 \\ 0.0005067064 \\ 0 \end{bmatrix}$$

The eigenvectors corresponding to this eigenvalues:

$$\begin{bmatrix} 0 & 0 & 0 & 0 & 0 & 0 & 0.0042 \\ 0.1689 & -0.2897 & 0.2858 & 0.1822 & 0.0714 & -0.0193 & -0.0464 \\ 0.5427 & -0.6350 & 0.2751 & -0.1503 & -0.2531 & 0.1465 & 0.2109 \\ 0.6799 & -0.2187 & -0.5147 & -0.5153 & 0.1350 & -0.4485 & -0.5062 \\ 0.4337 & 0.4339 & -0.6020 & 0.3489 & 0.4935 & 0.6884 & 0.6750 \\ 0.1583 & 0.4667 & 0.1034 & 0.5907 & -0.7569 & -0.5269 & -0.4725 \\ 0.0399 & 0.2428 & 0.4524 & -0.4561 & 0.3101 & 0.1597 & 0.1350 \end{bmatrix}$$

By choosing the eigenvector that corresponding to the eigenvalue 1, and normalising this eigenvector, yields:

$\lambda = 1$	Eigenvector
$p_3$	0
$p_4$	0.0834717
$p_5$	0.2682274
$p_6$	0.3360096
$p_7$	0.2143515
$p_8$	0.0782181
$p_9$	0.0197218
The sum	1

Table 8: Cell-edges distribution as represented by eigenvector corresponding to  $\lambda = 1$  in (N1) model.

This is the same results that were obtained from Newman's first model.

### 3.1.3 Newman's second model

The transition matrix  $(U)^T$  of Newman's second model: 4, 5, 6, 7, 8, 9-sided cells.

$$U^T = \begin{bmatrix} 0 & 0 & 0 & 0 & 0 & 0 \\ 1 & \frac{1}{2} & \frac{3}{10} & \frac{3}{16} & \frac{2}{17} & \frac{3}{41} \\ 0 & \frac{1}{2} & \frac{2}{5} & \frac{5}{16} & \frac{4}{17} & \frac{7}{41} \\ 0 & 0 & \frac{3}{10} & \frac{5}{16} & \frac{5}{17} & \frac{21}{82} \\ 0 & 0 & 0 & \frac{3}{16} & \frac{4}{17} & \frac{21}{82} \\ 0 & 0 & 0 & 0 & \frac{2}{17} & \frac{10}{41} \end{bmatrix}$$

The characteristic equation of the transition matrix:

$$\lambda^6 - \frac{94329 \lambda^5}{55760} + \frac{22043 \lambda^4}{27880} - \frac{22201 \lambda^3}{223040} + \frac{27 \lambda^2}{44608} - \frac{\lambda}{111520} = 0 \quad (3.3)$$

Solving equation 3.3, gives this eigenvalues:

$$Eigenvalues = \begin{bmatrix} 1.0000 \\ 0.4936 \\ 0.1925 \\ 0.0028 + 0.0093i \\ 0.0028 - 0.0093i \\ 0 \end{bmatrix}$$

The eigenvectors corresponding to this eigenvalues:

$$\begin{bmatrix} 0 & 0 & 0 & 0 & 0 & 0 \\ -0.5892 & 0.6145 & -0.3482 & 0.0282 + 0.0183i & 0.0282 - 0.0183i & 0.0197 \\ -0.7181 & 0.4557 & -0.0456 & 0.0209 - 0.0632i & 0.0209 + 0.0632i & 0.0414 \\ -0.3584 & -0.3564 & 0.7092 & -0.4567 + 0.0599i & -0.4567 - 0.0599i & -0.4725 \\ -0.0927 & -0.4853 & 0.2449 & 0.7950 + 0.0000i & 0.7950 + 0.0000i & 0.7927 \\ -0.0144 & -0.2286 & -0.5602 & -0.3873 - 0.0149i & -0.3873 + 0.0149i & -0.3824 \end{bmatrix}$$

By choosing the eigenvector that corresponding to the eigenvalue 1, and normalising this eigenvector, yields:

$\lambda = 1$	Eigenvector
$p_4$	0
$p_5$	0.332345
$p_6$	0.405067
$p_7$	0.202159
$p_8$	0.052293
$p_9$	0.008137
The sum	1

Table 9: Cell-edges distribution as represented by eigenvector corresponding to  $\lambda = 1$  in (N2) model.

This is the same results that were obtained from Newman's second model.

### 3.1.4 Newman's third model

The transition matrix  $(U)^T$  of Newman's third model: 3, 4, 5, 6, 7, 8, 9-sided cells.

$$U^T = \begin{bmatrix} 0 & 0 & 0 & 0 & 0 & 0 & 0 \\ \frac{1}{2} & \frac{2}{7} & \frac{1}{6} & \frac{3}{31} & \frac{1}{18} & \frac{4}{127} & \frac{3}{170} \\ \frac{1}{2} & \frac{3}{7} & \frac{1}{3} & \frac{15}{62} & \frac{1}{6} & \frac{14}{127} & \frac{6}{85} \\ 0 & \frac{2}{7} & \frac{1}{3} & \frac{10}{31} & \frac{5}{18} & \frac{28}{127} & \frac{14}{85} \\ 0 & 0 & \frac{1}{6} & \frac{15}{62} & \frac{5}{18} & \frac{35}{127} & \frac{21}{85} \\ 0 & 0 & 0 & \frac{3}{31} & \frac{1}{6} & \frac{28}{127} & \frac{21}{85} \\ 0 & 0 & 0 & 0 & \frac{1}{18} & \frac{18}{127} & \frac{43}{170} \end{bmatrix}$$

The characteristic equation of the transition matrix:

$$\lambda^7 - \frac{14126821 \lambda^6}{8433054} + \frac{48917167 \lambda^5}{63247905} - \frac{16879279 \lambda^4}{168661080} + \frac{30713 \lambda^3}{14881860} + \frac{\lambda^2}{453390} + \frac{\lambda}{63247905} = 0 \quad (3.4)$$

Solving equation 3.4, gives this eigenvalues:

$$Eigenvalues = \begin{bmatrix} 1.0000 \\ 0.4855 \\ 0.1770 \\ 0.0311 \\ -0.0004 + 0.0032i \\ -0.0004 - 0.0032i \\ 0 \end{bmatrix}$$

The eigenvectors corresponding to this eigenvalues:

$$\begin{bmatrix} 0 & 0 & 0 & 0 & 0 & 0 & 0.0146 \\ 0.2574 & -0.3837 & 0.3134 & -0.1530 & -0.0227 + 0.0239i & -0.0227 - 0.0239i & 0 \\ 0.5447 & -0.5659 & 0.1730 & 0.1745 & 0.0236 - 0.1223i & 0.0236 + 0.1223i & -0.1816 \\ 0.6356 & -0.2348 & -0.3760 & 0.2758 & 0.2345 + 0.1798i & 0.2345 - 0.1798i & 0.1941 \\ 0.4364 & 0.3408 & -0.6242 & -0.0192 & -0.6514 + 0.0000i & -0.6514 + 0.0000i & 0.4133 \\ 0.1942 & 0.4736 & -0.0662 & -0.7837 & 0.6226 - 0.1787i & 0.6226 + 0.1787i & -0.7952 \\ 0.0693 & 0.3700 & 0.5800 & 0.5055 & -0.2067 + 0.0974i & -0.2067 - 0.0974i & 0.3548 \end{bmatrix}$$

By choosing the eigenvector that corresponding to the eigenvalue 1, and normalising this eigenvector, yields:



$\lambda = 1$	Eigenvector
$p_3$	0
$p_4$	0.120428
$p_5$	0.254817
$p_6$	0.297341
$p_7$	0.204161
$p_8$	0.090838
$p_9$	0.032416
The sum	1

Table 10: Cell-edges distribution as represented by eigenvector corresponding to  $\lambda = 1$  in (N3) model.

And this is the same results that were obtained from Newman's third model.

### 3.2 Conclusion

As noted in the results of the previous models as  $t \rightarrow \infty$  it converge to zero and this caused by the leak of transition matrix in each model. To be more specific, if the model represent the cells with 4, 5, 6, 7, 8, 9 edges after one round of division, the 9-sided cell will be lost from the transition matrix and this caused by the role of the  $S$  matrix, which imposed that each cell will gain one extra edge after one round of division, or in another word the probability of 9-sided cell to remain 9-sided cell = 0. Fixing this term will eliminate the leak by eliminating the increase of the 9-sided cell (9-sided cell will not pick up an extra edge from dividing neighbour) this ensure that this type of the cells will not be lost from the transition matrix after the division. In addition, finding the results of the models by solving eigen-problems is more efficient mathematically. In the previous models as  $t \rightarrow \infty$  every time they obtained values needed to be normalised to avoid the convergence to zero. However, by finding the eigen-values of the transition matrices of the models and choosing the eigen-vector which corresponding to the eigen-values 1 or an approximate to 1. This vector in every model represents the result of the model without the need to normalise the obtained vector.

**Example.**

By extending the transition matrix of Gibson's model to be  $(9 \times 9)$  matrix instead of  $(7 \times 7)$ .

$$\begin{bmatrix} 0 & 0 & 0 & 0 & 0 & 0 & 0 & 0 & 0 \\ 1 & \frac{1}{2} & \frac{1}{4} & \frac{1}{8} & \frac{1}{16} & \frac{1}{32} & \frac{1}{64} & \frac{1}{128} & \frac{1}{256} \\ 0 & \frac{1}{2} & \frac{1}{2} & \frac{3}{8} & \frac{1}{4} & \frac{5}{32} & \frac{3}{32} & \frac{7}{128} & \frac{1}{32} \\ 0 & 0 & \frac{1}{4} & \frac{3}{8} & \frac{3}{8} & \frac{5}{16} & \frac{15}{64} & \frac{21}{128} & \frac{7}{64} \\ 0 & 0 & 0 & \frac{1}{8} & \frac{1}{4} & \frac{5}{16} & \frac{5}{16} & \frac{35}{128} & \frac{7}{32} \\ 0 & 0 & 0 & 0 & \frac{1}{16} & \frac{5}{32} & \frac{15}{64} & \frac{35}{128} & \frac{35}{128} \\ 0 & 0 & 0 & 0 & 0 & \frac{1}{32} & \frac{3}{32} & \frac{21}{128} & \frac{7}{32} \\ 0 & 0 & 0 & 0 & 0 & 0 & \frac{1}{64} & \frac{7}{128} & \frac{7}{64} \\ 0 & 0 & 0 & 0 & 0 & 0 & 0 & \frac{1}{128} & \frac{1}{32} \end{bmatrix}$$

The Eigenvalues of this matrix are:

$$[1.0000, 0.5000, 0.2500, 0.1247, 0.0594, 0.0222, 0.0044, 0.0002, 0]$$

And the Eigenvector corresponding to the Eigen value 1 is:

$$[0, 0.2888, 0.4640, 0.2085, 0.0359, 0.0027, 0.00009, 0.000002, 1.239753^{-8}]$$

The main point is no matter what is the size of the transition matrix. The results will be always represented or delivered in the Eigenvector corresponding to the Eigenvalue 1 or approximate to 1.

## Chapter 4

# Fitting the experimental histogram to commonly used probability density functions.

The aim of this section is to find if there is a probability density functions that can describe the data that were obtained from the actual observation as shown in Figure 2.2. Also, the purpose of this procedure is to find the closest fit, which can lead to predicting the frequency of occurrence (the pattern) of the phenomenon in a certain period.

There are many probability distribution functions that were examined to fit the histogram which represents the actual data. A closer fit depends on the distribution function and the histogram's characteristic.

### 4.1 Poisson distribution

The first probability function that were examined is Poisson function.

$$P(x) = \frac{\lambda^x}{x!} * e^{-\lambda} \quad (4.1)$$

where,

( $e$ ) is Euler's number ( $e = 2.71828\dots$ ) and ( $x!$ ) is the factorial of  $x$ .

Poisson distribution was chosen in the first place because of many reasons, besides the similarity of the shape of the histograms, the fact that many of this distribution assumptions have been satisfied. For instance

- [1] ( $x$ ) which represent the number of the edges is a positive integer ( $x \geq 0$ ).
- [2] Events occur independently.
- [3] The variance between the events is constant.

Consider  $x$  as the number of edges which will represent the  $x$ -axis, the frequency of the events which will be described by  $Y$  - axis and  $\lambda$  is the average number of events per interval also known as the rate parameter.

Choosing  $x = 0, 1, 2, 3, 4, 5$  corresponding to the number of the edges 4, 5, 6, 7, 8, 9 respectively. And  $\lambda = 2$  which represent the mean.

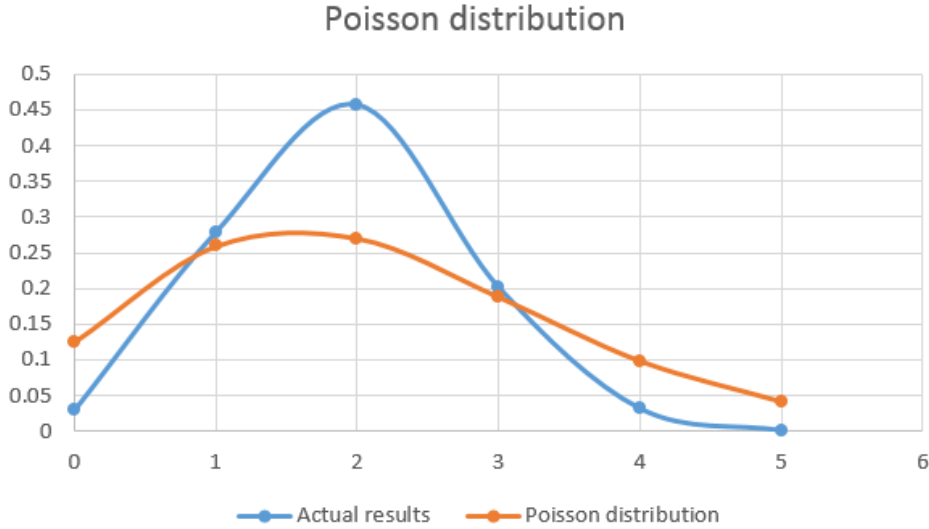


Figure 4.1: Plots of the experimental histogram (Blue) and the fitted Poisson’s histogram (Orange), by using non-linear squares curve fitting with Microsoft Excel Solver.

$x$	$Y_{OBS}$	$Y_{CALC}$	$(Y_{OBS} - Y_{CALC})^2$
0	0.02946593	0.124353845	0.009003716
1	0.279005525	0.259231034	0.000391031
2	0.45718232	0.270199641	0.034962522
3	0.201197053	0.187754902	0.000180691
4	0.031767956	0.097849602	0.004366784
5	0.001381215	0.04079593	0.00155352
The sum	1	0.980184955	0.050458264

Table 11: Values of cell-edges distribution obtained by Poisson distribution.

Running the solver programme to define the minimum value for the target cell (the sum of  $(Y_{OBS} - Y_{CALC})^2$ ) by changing the value of  $\lambda$  yields:

$$\lambda = 2.0846241846991$$

According to Figure (4.4), and the error that was obtained from attempting to fit Poisson distribution to the histogram (0.050458264), one may argue that Poisson distribution did not agree well with the histogram. Thus, this distribution can not be used to expect or to determine the pattern of the division and proliferation of the epithelial cells.

## 4.2 Normal distribution

One of the most common distributions that were used in the natural and social sciences to describe random variables whose distributions are not known is the normal (or Gaussian) distribution. The shape of the histogram (The Bell Curve) is Similar to the normal distribution curve. Furthermore, the method (least squares parameter fitting) can be derived analytically in explicit form when the relevant variables are normally distributed. Hence, the normal distribution was examined to fit the actual data.

$$f(x, \mu, \sigma) = \frac{1}{\sigma\sqrt{2\Pi}} * e^{-\frac{(x-\mu)^2}{2\sigma^2}} \quad (4.2)$$

Where:  $x$  in this case represents is the number of the edges.

$\mu$  is the mean.

$\sigma$  is standard deviation.

$\sigma^2$  is variance.

$x$	$Y_{OBS}$	$Y_{CALC}$	$(Y_{OBS} - Y_{CALC})^2$
4	0.02946593	0.042180954	0.000161672
5	0.279005525	0.272934875	$3.68528E - 05$
6	0.45718232	0.459031525	$3.41956E - 06$
7	0.201197053	0.20066279	$2.85438E - 07$
8	0.031767956	0.022799852	$8.04269E - 05$
9	0.001381215	0.000673346	$5.0108E - 07$
The sum	1	0.998283341	0.000283158

Table 12: Values of cell-edges distribution obtained by Normal distribution.

Using the method (least squares parameter fitting) yields:

$$\mu = 5.885849699, \sigma = 0.86149975$$

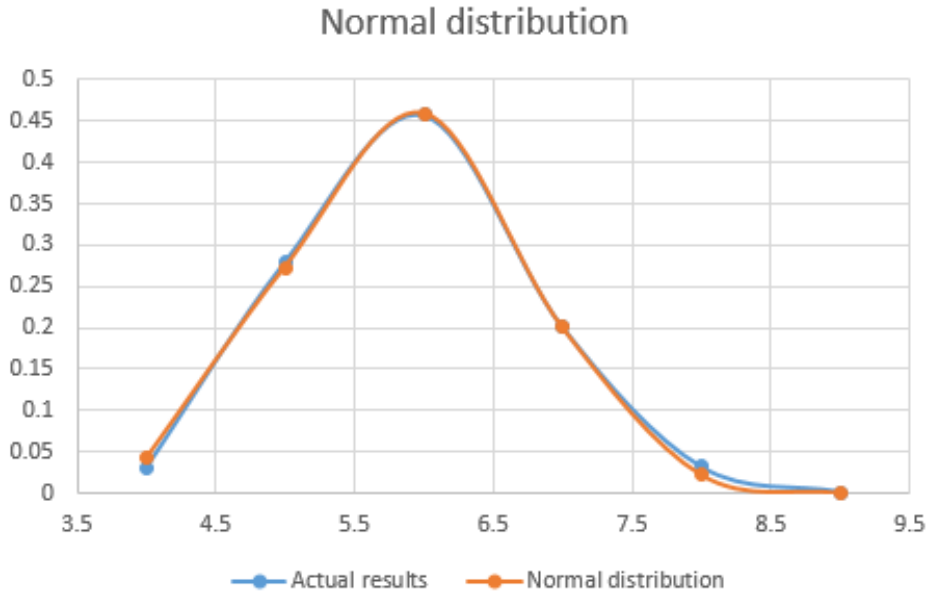


Figure 4.2: Plots of the experimental histogram (Blue) and the fitted Normal histogram (Orange), by using non-linear squares curve fitting with Microsoft Excel Solver.

Checking: The curve peaked where,

$$f(x, \mu, \sigma) = \frac{1}{\sigma\sqrt{2\Pi}} \Rightarrow e^{-\frac{(x-\mu)^2}{2\sigma^2}} = 1$$

Which means

$$-(x - \mu)^2 = 0 \Rightarrow x = \mu \Rightarrow 6 \approx 5.885849699$$

According to Figure(4.2), the Normal distribution has shown better agreement Consistent with the experimental data. However, there are a couple of drawbacks of such distribution which cannot be neglected in this case such as, the normal distribution curve is symmetrical while the experimental data is not. Moreover, the fact that  $x \in \mathbb{R}$  in the normal distribution whereas  $x$ , which represent the number of the edges, must be a positive integer.

### 4.3 Log-normal distribution

Considering the excellent match between the curves in the prior distribution. The gaps of the distribution which are not consistent with the data, this strongly suggested the Log-normal distribution.

$$\ln f(x, \mu, \sigma) = \frac{1}{x\sigma\sqrt{2\Pi}} * e^{-\frac{(\ln x - \mu)^2}{2\sigma^2}}, x > 0 \quad (4.3)$$

$x$	$\ln x$	$Y_{OBS}$	$Y_{CALC}$	$(Y_{OBS} - Y_{CALC})^2$
4	1.386294361	0.02946593	0.018021356	0.000130978
5	1.609437912	0.279005525	0.281487086	6.15815E - 06
6	1.791759469	0.45718232	0.456743238	1.92793E - 07
7	1.945910149	0.201197053	0.199803777	1.94122E - 06
8	2.079441542	0.031767956	0.039083456	5.35165E - 05
9	2.197224577	0.001381215	0.004577233	1.02145E - 05
The sum		1	0.999716147	0.000192787

Table 13: Values of cell-edges distribution obtained by Log-normal distribution.

Using the least squares parameter fitting technique yields,

$$\mu = 1.777282518, \sigma = 0.144849707$$

Checking: The curve peaked where,

$$\ln f(x, \mu, \sigma) = \frac{1}{x\sigma\sqrt{2\Pi}} \Rightarrow e^{-\frac{(\ln x - \mu)^2}{2\sigma^2}} = 1$$

Which means

$$-(\ln x - \mu)^2 = 0 \Rightarrow \ln x = \mu \Rightarrow x = e^\mu \Rightarrow 6 \approx 5.913764014$$

Besides the fact that the log-normal distribution meets the terms of the experimental data from where it only contains positive integers and the histogram of such distribution is asymmetric. This type of distribution was found in a similar case. Lognormal distribution represent the distribution of the metal and gold values, this claimed by Razumovsky[14], who inspired Kolmogorov to do extra research and studies to investigate the truth of such claim and thus he reached another similar case. According to Kolmogorov[12], lognormal law for distribution determines the sizes of crushed particles.

Let:  $N(t)$  = Number of particles at time  $t$ .  $N(r, t)$  = Number of particles with size  $x$  lesser than  $r$ .

Distribution function:

$$P(x < r) = \frac{N(r, t)}{N(t)} \quad (4.4)$$

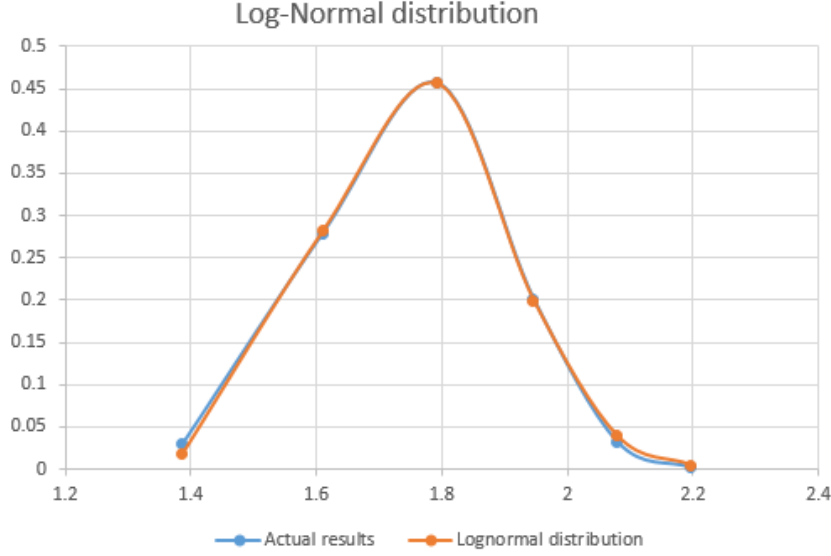


Figure 4.3: Lognormal distribution curve (Orange) adequately describes the experimental data (Blue) by using non-linear squares curve fitting with Microsoft Excel Solver.

After crushing the particles occurring at  $(t, t + 1)$ :

$Q(k)$  is the expected number of new particles from particles of size  $r$ .

$Q(k, r)$  the number of particles with size  $x$  lesser than  $k.r$ .

Repeating the process many times (As  $t \rightarrow \infty$ ):

$$p(x) = \frac{N(e^x, t)}{N(t)} \rightarrow \frac{1}{\sqrt{2\pi t} B} \int_{-\infty}^x e^{-\frac{(\xi - At)^2}{2B^2 t}} d\xi \quad (4.5)$$

Where,

$$A = \frac{1}{Q(1)} \int_0^1 \text{Log } k \, dQ(k)$$

And,

$$B^2 = \frac{1}{Q(1)} \int_0^1 (\text{Log } k - A)^2 \, dQ(k)$$

$$\boxed{\mu = At; \sigma = B\sqrt{t}}$$

*Note.* Although the log-normal distribution shows a better approximation and the histogram is almost lookalike the experimental data histogram, the log-normal distribution is a continuous function while the actual data is not a continuous.

## 4.4 Conclusion

Regardless the fact that log-normal distribution shows a remarkable similarity which is almost identical according to the histogram (4.3). There is a fact which cannot be overlooked that is the log-normal is a continuous function, whereas the actual data is not continuous. The histogram of the experimental data, which represent

the distribution of the cells, was based on the number of (edges-vertices-neighbours) of the cell. Therefore, it cannot be considered continuous function. And this might explain the slight difference between the histograms. Perhaps if the experimental histogram was based on the size of the cell rather than the number of the edges, in this case, the distribution function considered as continuous function and might be identical to the lognormal distribution.

## length histogram

This function plots a histogram of the length of all the cells in a population.

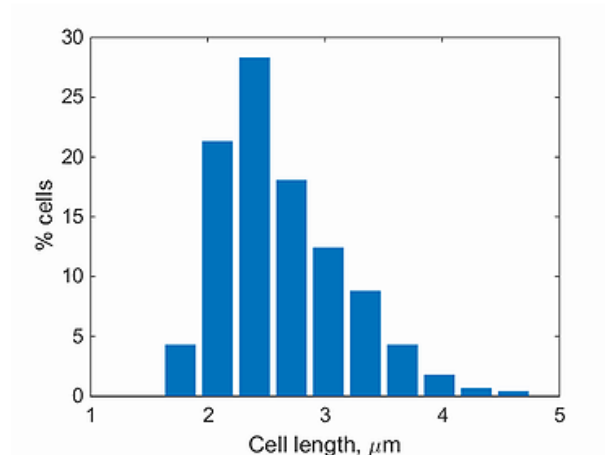


Figure 4.4: Histogram for cell-length distribution [15].



# Chapter 5

## Future work

Perhaps a good start for the future work is by modelling virtual tissues and compare the histogram of each model with the histograms of experimental and the previous models as well. Such an idea will be presented in the main dissertation. To briefly introduce the structure of this design, two different types of virtual tissues will be introduced:

### **Virtual model for growing tissue.**

Virtual model for growing tissue will be based on several assumptions that tissue topology emerges from cellular division.

The assumptions of this model:

- a) Start with one cell ( $n = 1$ ).
- b) Divide through two random (not adjacent) edges.
- c) Repeat picking up random neighbour.
- d) If  $n \geq 3$  then pick up randomly two other cells and add extra edge to them.

Repeating this process (the division) for example 1000 times and translate the obtained data from 1001 cells into a histogram. Finally, compare this histogram to the other histograms.

### **Topology emerging from T1 transitions.**

This model differs from the previous regarding the concepts. This model is not about cell division; it takes into account cell elasticity and junctional forces arising from adhesion as shown in Figure( 5.1). Translating this numerically. Thus, generate different network morphologies that depend on physical parameters [16].

The assumptions of this model:

- a) Start with  $n$  hexagonal cells. ( $n = 1000$ ) for instance.

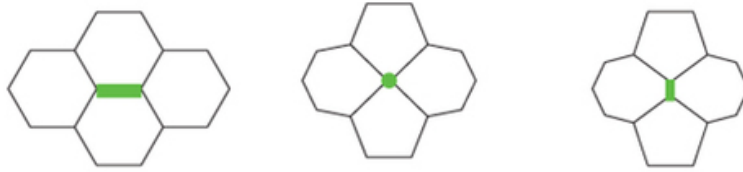


Figure 5.1: Cells undergoing a T1 topological swap. The green edge shows the cell-cell interface that is shrunk to a point and then transformed in the perpendicular direction. [4].

- b) Randomly select two cells (acting as two neighbours undergoing T1 transition) and reduce the number of their edges by one each.
- c) Choose two other random cells assuming they are neighbours and add one extra edge to each.

Repeat the process N times, then translate the obtained data into a histogram. Finally, compare this histogram to the other histograms.

# Bibliography

- [1] DeMill, Colin. 'Epithelial Tissue'. Uoguelph.ca. N.p., 2015. Web. 29 Nov. 2015.
- [2] Gibson, M., Patel, A., Nagpal, R. and Perrimon, N. (2006). The emergence of geometric order in proliferating metazoan epithelia. *Nature*, **442(7106)**, pp.1038–1041.
- [3] Lecuit, Thomas. *Tissue Remodeling And Epithelial Morphogenesis*. San Diego: Elsevier/Academic Press, 2009. Print.
- [4] Nature.com, (2015). *Nature Publishing Group: science journals, jobs, and information*. [online] Available at: <http://www.nature.com/index.html> [Accessed 8 Dec. 2015].
- [5] Patel, Ankit B. et al. 'Modeling And Inferring Cleavage Patterns In Proliferating Epithelia'. *PLoS Comput Biol* **5.6** (2009): e1000412. Web.
- [6] Rogers., (1983). *Cells and Tissues*. Oxford: Elsevier Science.
- [7] Sandersius SA, Chuai M, Weijer CJ, Newman TJ (2011) Correlating Cell Behavior with Tissue Topology in Embryonic Epithelia. *PLoS ONE* **6(4)**: e18081. doi:10.1371/journal.pone.0018081
- [8] Harris, C., Trump, B. and Stoner, G. (1980). Normal human tissue and cell culture. New York: Academic Press.
- [9] Campbell, N., Reece, J. and Simon, E. (2004). Essential biology. San Francisco: Pearson/Benjamin Cummings.
- [10] Fried, G., Hademenos, G. and Fried, G. (2013). Biology. New York: McGraw-Hill Education.
- [11] Nidcd.nih.gov. (2016). Chain reaction: NIH researchers find dynamic ties between epithelial cells — NIDCD. [online] Available at: <https://www.nidcd.nih.gov/news/2013/chain-reaction-nih-researchers-find-dynamic-ties-between-epithelial-cells> [Accessed 12 May 2016].
- [12] Kolmogorov, A. N. *On the log-normal distribution of particles sizes during break-up process* // Dokl. Akad. Nauk. **SSSR XXXI 2**, 99–101, 1941.
- [13] Nagpal, R., Patel, A. and Gibson, M. (2008). Epithelial topology. *Bioessays*, **30(3)**, pp.260-266.

- [14] Razumovsky NK. 1940. *Distribution of metal values in ore deposits*. Comptes
- [15] Rendus (Doklady) de l'Académie des Sciences **de l'URSS** 9: 814–816. Azzam, T., Evergreen, S., Germuth, A. and Kistler, S. (2013). Data Visualization and Evaluation. *New Directions for Evaluation*, 2013(139), pp.7-32.
- [16] Farhadifar, R., Roper, J., Aigouy, B., Eaton, S. and Jlicher, F. (2007). *The Influence of Cell Mechanics, Cell-Cell Interactions, and Proliferation on Epithelial Packing*. **Current Biology**, 17(24), pp.2095–2104.